

Study the Effect of Substitution La^{+3} Ion on the Structural and Electrical Properties of the Prepared Nano-Ferrite($\text{Ni}_{0.3}\text{Cu}_{0.2}\text{Zn}_{0.5}\text{Fe}_{2-x}\text{O}_4$)

Abdul Majeed Rafeek Ahmed
Rusul Alaa Najem

Dept. Of Physics/college of Education for pure science – Ibn Al-Haitham / University of Baghdad

Abstract

Nano ferrite with chemical formula ($\text{Ni}_{0.3}\text{Cu}_{0.2}\text{Zn}_{0.5}\text{La}_x\text{Fe}_{2-x}\text{O}_4$), were prepared by using sol-gel auto-combustion method for the values of ($x=0.0, 0.025, 0.05$ and 0.075). The prepared samples were calcined at (900°C) for (2h). The structural characterizations of resulting ferrite were examined by x-ray diffraction (XRD) and scanning electron microscope (SEM) techniques. XRD results showed that the resulting ferrite possess a spinel cubic phase with a particle size ranging from (23-36nm). We found that the Lattice constants and density ($\rho_{x\text{-ray}}$) increases with increasing La^{+3} content, while the porosity was found to be to decreases with increasing La^{+3} content. The frequency dependent dielectric properties have been studied by (LCR meter) device. The results revealed that the values of the dielectric constant and the dielectric loss factor decreases by increasing frequency. The increase in alternating conductivity ($\sigma_{a.c}$) was also observed with increasing frequency.

Keywords:- La^{+3} ions; Ferrites; sol-gel method; XRD; SEM; Dielectric Parameters.

1. Introduction

Ferrites nano particles are of great interest because of their scientific aspect and several applications. The Nano ferrites are interesting materials owing to their wide range of applications in new science and technology [1]. The structural and magnetic properties of spinel ferrites depend on the magnetic interaction and cation distribution in the two sub-lattices *i.e.* Tetrahedral (A) and octahedral (B) lattice sites [2]. The Electrical properties of ferrites are dependent on the microstructure, chemical composition and synthesis technique [3]. Several methods are used for synthesising nanosized spinel ferrites such as co-precipitation, sol-gel, micro-emulsion, hydrothermal, and reverse micelle methods [4,5]. NICUZN ferrite is the most suitable one in which the magnetic and electrical properties are affected by the substituent [6]. Rare earth materials are known to possess good electrical insulation properties with high electrical resistivity. Therefore, the substitution of these rare earth ions into spinel ferrites could alter the electrical and magnetic properties. Moreover, these rare earth ions have a huge influence on the magnetic anisotropy of the system making the spinel ferrite as promising materials replacing the Hexaferrite or garnets [7, 8].

II. EXPERIMENTAL

The ferrite powders are synthesised through a nitrate-citrate auto-combustion method for achieving homogenous mixing of the component on the atomic scale and better sinter ability of synthesised

powder [9]. Analytical grade nickel nitrate $[\text{Ni}(\text{NO}_3)_2 \cdot 6\text{H}_2\text{O}]$, zinc nitrate $[\text{Zn}(\text{NO}_3)_2 \cdot 6\text{H}_2\text{O}]$, copper nitrate $[\text{Cu}(\text{NO}_3)_2 \cdot 3\text{H}_2\text{O}]$, iron nitrate $[\text{Fe}(\text{NO}_3)_3 \cdot 9\text{H}_2\text{O}]$, citric acid $[\text{C}_6\text{H}_8\text{O}_7 \cdot \text{H}_2\text{O}]$ and lanthanum nitrate $[\text{La}(\text{NO}_3)_3]$ were used to prepare $(\text{Ni}_{0.3} \text{Cu}_{0.20} \text{Zn}_{0.5}) \text{La}_x \text{Fe}_{2-x} \text{O}_4$ ferrite with $x = 0.0, 0.025, 0.050$ and 0.075 compositions. Metal nitrates and citric acid were dissolved in deionized water, all these are collected in a glass beaker and mixed well at room temperatures by hot plate magnetic stirrers with high speed, Ammonia solution was added slowly the form of drops into the mixed solution to control its pH until reach threats from 7 with continuous rotation. Gradually increase in temperature to reaches of 80°C to transform it into a gel and then ignited in a self-propagating combustion manner to form a fluffy loose powder The as-burnt precursor powder was then calcined at 900°C for 2 h. The powder was pressed using a die with a diameter (1.5cm) to produce specimens in a pellet shapes. The pressing load used was (7ton) and the specimens held for 1min under pressure using a hydraulic press of a maximum load 15ton.

III. Results and Discussion

A - X-Ray Diffraction Results:

XRD patterns of $(\text{Ni}_{0.3} \text{Cu}_{0.20} \text{Zn}_{0.5}) \text{La}_x \text{Fe}_{2-x} \text{O}_4$ Nano crystals, for all the samples with $x = 0.00, 0.025, 0.050$, and 0.075 are shown in Fig 1. The X-ray diffraction patterns reveal a single-phase cubic spinel structure with few traces of secondary phase. Furthermore, the observed diffraction peaks could be assigned to the reflection plane of (111), (220), (311), (400), (422), (511) and (440) which could be indexed to a single-phase Ni-Cu-Zn ferrite Nano crystal [10]. Meanwhile, the peak corresponding to $2\theta = 32.21$ is attributed to secondary phase at the grain boundaries for (\star) LaFeO_3 (ICDD PDF #7142203) except for the cubic spinel phase. The intensity of LaFeO_3 peak has increased with the increase in La^{+3} -ion concentration. Furthermore, another secondary phase of [11-12 -13].

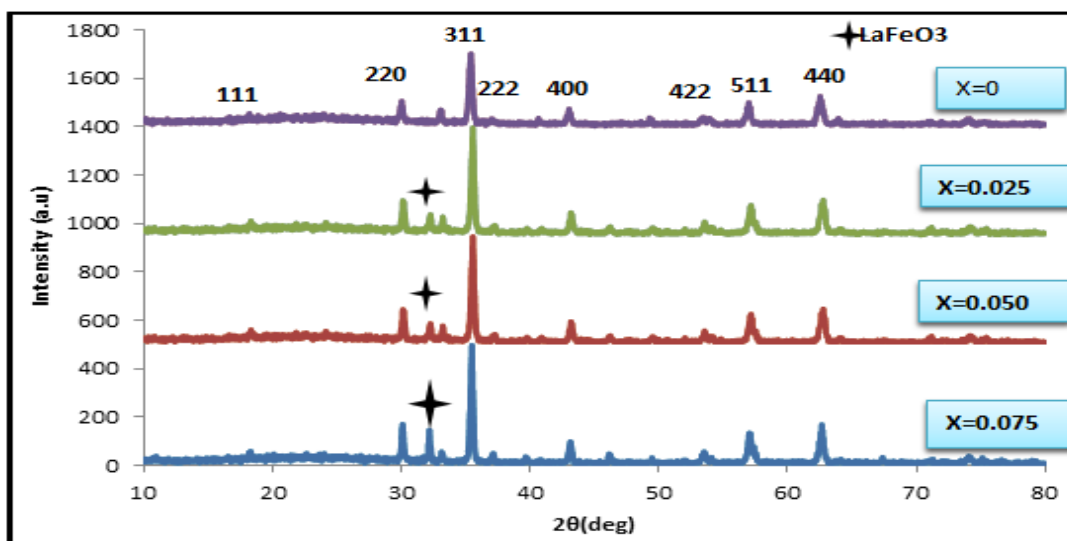


Fig 1 XRD diffraction patterns for the sample of $\text{Ni}_{0.3} \text{Cu}_{0.2} \text{Zn}_{0.5} \text{La}_x \text{Fe}_{2-x} \text{O}_4$

The lattice parameter of individual composition was investigated by using the following relation: [14].

$$d_{hkl} = \frac{a}{\sqrt{h^2 + k^2 + l^2}} \dots \dots \dots (1)$$

Where 'a' is the lattice constant, d is the inter-planar distance and (h, k, l) are the Miller indices

The average crystallite size of the sample is determined using the Scherer's equation [15].

$$\dots \dots \dots (2) \quad D = \left(\frac{K\lambda}{\beta_{hkl} \cos \theta} \right)$$

where D is the crystallite size, β is the full width of the diffraction line at half of the maximum intensity measured in radians, λ is x-ray wavelength (Cu k α radiation, 1.5405Å) and θ is the Bragg angle. ϵ and Williamson-Hall formula

$$\beta_{hkl} \cos \theta = \frac{K\lambda}{D} + [4\epsilon \sin \theta] \dots \dots \dots (3)$$

The actual (X-ray) density of the samples was calculated using the formula [16]:

$$\rho_{x\text{-ray}} = \frac{ZM_{wt}}{N_a V} \dots \dots \dots (4)$$

Where M is the molecular weight (Kg) of the sample, N is Avogadro's number (per mol) and a is the lattice parameter (Å). Bulk densities of the samples were determined using the formula:

$$\rho_b = \frac{m}{\pi r^2 h} \dots \dots \dots (5)$$

Where m is the mass (Kg), r is the radius (m) and h is the height of the pellet (m).

Percentage of porosity was calculated using the following formula [17]

$$P = 1 - \frac{\rho}{\rho_{x\text{-ray}}} \times 100\% \dots \dots \dots (6)$$

Table 1: Effect of La⁺³ doping on the lattice parameter, crystallite size, actual (X-ray) density, Bulk density, porosity of (Ni_{0.3} Cu_{0.20} Zn_{0.5}) La_xFe_{2-x}O₄ system

Sample	X Content	Lattice Constant (a)	D _{Sh} (nm)	D _{w-h} (nm)	$\rho_{x\text{-ray}}$ (g/cm ³)	ρ (g/cm ³)	Porosity %
B0	0	8.3965	23.7673	25.8061	5.343933	3.470443	35.05826
B1	0.025	8.3985	29.4582	31.6917	5.353933	3.77568	31.42254
B2	0.050	8.3680	29.0249	34.6635	5.505971	3.775855	29.99077
B3	0.075	8.3815	36.3581	39.5156	5.539952	3.878478	29.47839

The observed increase in the lattice constant (a) which could be associated with the increasing La^{+3} content where the ionic radius of La^{+3} (1.6061) is bigger than that of Fe^{+3} ion (0.645) replacing iron ions on octahedral B-site which causes asymmetry in the structure. Hence, the lattice constant should be aggrandized with the increasing content of the La^{+3} during the substitution process [18,19]. Besides that, the decrease in lattice constant with the increase of La^{+3} content could be attributed to the compression of spinel lattice induced by the secondary phases due to the difference in thermal expansion coefficients [18,20]. The crystallite size of the samples is observed to increase with lanthanum concentration. This is consistent with the results reported for La^{+3} doped Ni-Cu-Zn ferrite [21]. The X-ray density increases linearly with lanthanum ion content and this can be correlated with the increase of atomic weight of La^{+3} substituted for Fe^{+3} of lower atomic mass. The magnitudes of bulk densities are smaller than that of the corresponding X-ray densities and this difference in magnitude may be attributed to the existence of pores in the bulk samples. The porosity is observed to decrease with La^{+3} content.

B. SEM and EDX analysis

The SEM images of various compositions of NiCuZnLa ferrites were shown in the figure 2. The SEM images reveal that the particles are spherical in shape and are agglomerated in nature. Figure 3 shows the EDX images of all $(\text{Ni}_{0.3}\text{Cu}_{0.20}\text{Zn}_{0.5})\text{La}_x\text{Fe}_{2-x}\text{O}_4$ ($x = 0.00, 0.025, 0.050, \text{ and } 0.075$) ferrite nanoparticles calcined at 900°C . The characteristic peaks of Ni, Cu, Zn, La, Fe and O elements were observed in EDX spectra.

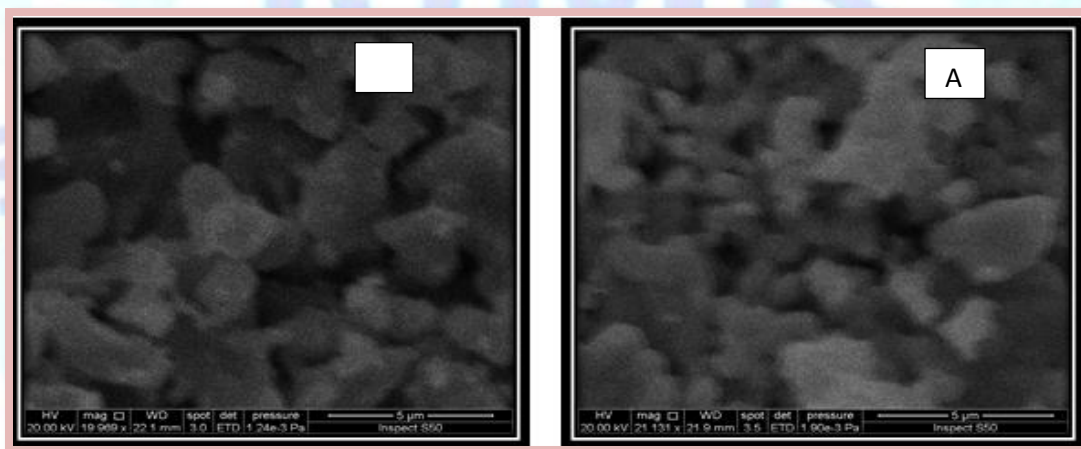


Fig.2. SEM photographs of $(\text{Ni}_{0.3}\text{Cu}_{0.20}\text{Zn}_{0.5})\text{La}_x\text{Fe}_{2-x}\text{O}_4$ ferrites with (A) $x = 0.00$, (B) $x = 0.075$.

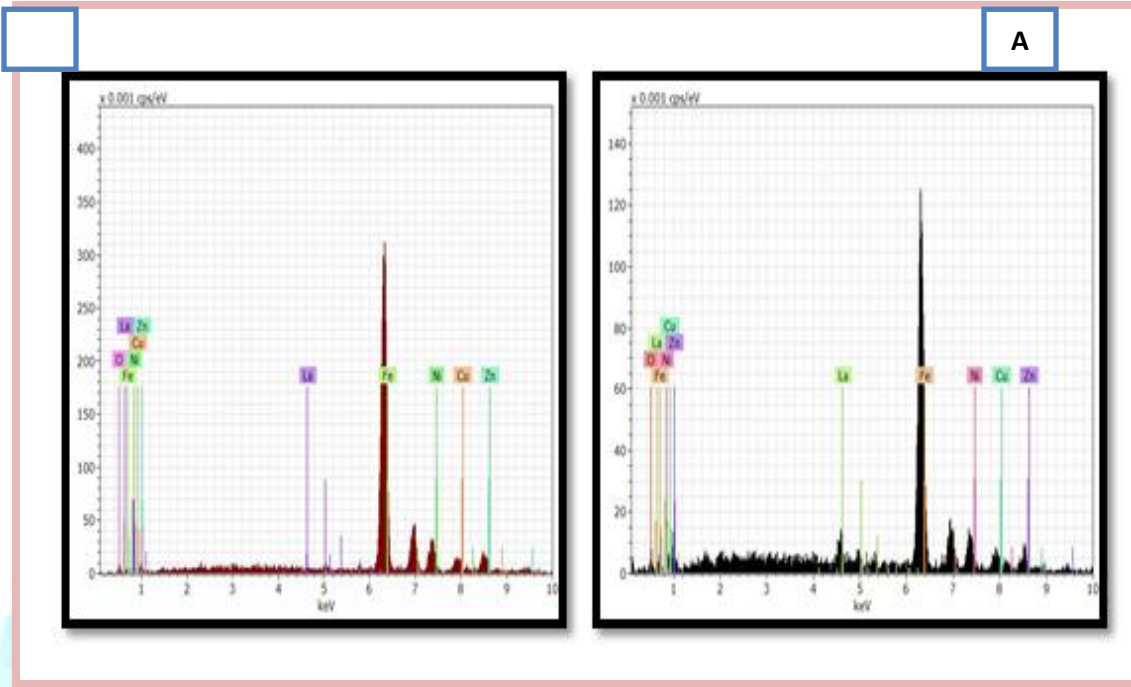


Figure3. EDX pattern $(Ni_{0.3}Cu_{0.20}Zn_{0.5})La_xFe_{2-x}O_4$ ferrite nanoparticles with (A) $x = 0.00$, (B) $x = 0.075$.

C. Electrical Properties

The electrical properties of La doped NiCuZn ferrite $(Ni_{0.3}Cu_{0.2}Zn_{0.5}Fe_{2-x}O_4)$, with $(X=0.0, 0.025, 0.05$ and $0.075)$ of Lanthanum additions include the a.c conductivity, dielectric properties.

A. Dielectric properties

The real part of the dielectric constant ϵ_r' was calculated by using the relation [22],

$$\epsilon_r' = \frac{c t}{\epsilon_0 A} \dots \dots \dots (7)$$

Where C is the measured value of capacitance, d is the thickness in centimetres, A is the surface area in square centimetres, ϵ_0 is dielectric permittivity of air (8.854×10^{-14} F/cm). The imaginary part of the dielectric loss ϵ_r'' was calculated by using the relation [22],

$$\epsilon_r'' = \tan \delta \epsilon_r' \dots \dots \dots (8)$$

Figures 4 and 5 show the dependence of the real and imaginary part of dielectric constant ϵ_r' , ϵ_r'' , for bulk $(Ni_{0.3}Cu_{0.20}Zn_{0.5})La_xFe_{2-x}O_4$ on the frequency ω , for different lanthanum doping contents. The real and imaginary parts of dielectric constant for all samples decrease with increasing of frequency. This behavior agrees well with Deby's type relaxation process. The real and imaginary parts of dielectric constant reach a constant value for all the samples above certain greater frequency, this agrees with the result of references [23]. It can be observed from Figures 4 that the imaginary parts of dielectric constant ϵ_r'' , increases with frequency.

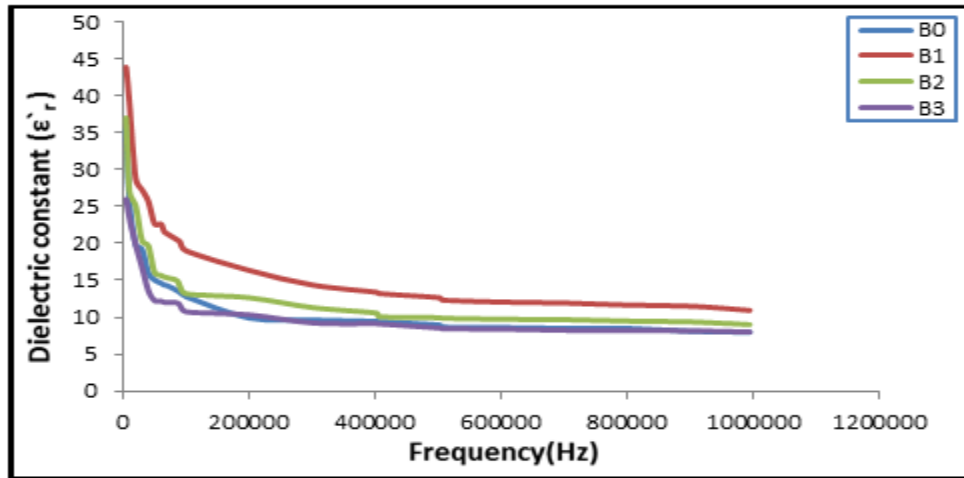


Figure4: Variation of real part (ϵ'_r) of dielectric constant with frequency for $(\text{Ni}_{0.3} \text{Cu}_{0.20}\text{Zn}_{0.5}) \text{La}_x\text{Fe}_{2-x}\text{O}_4$ at different La contents.

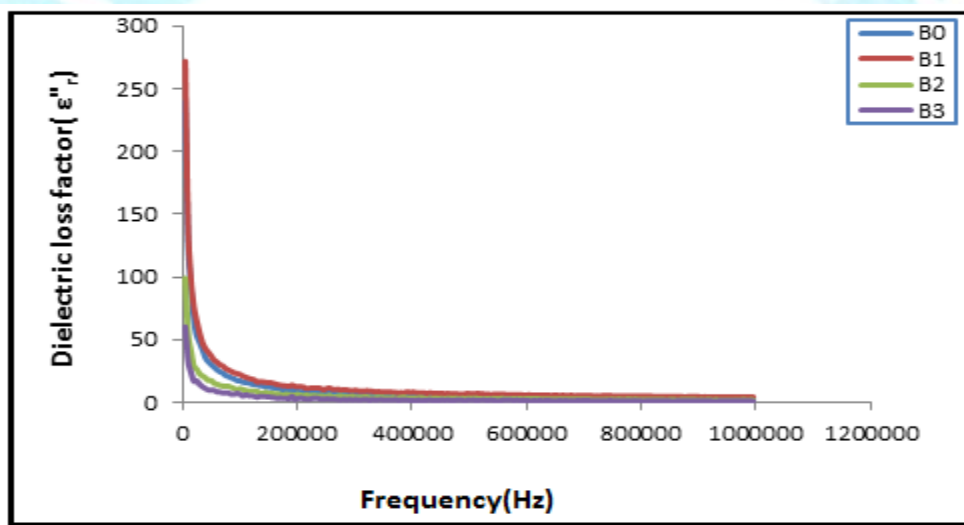


Figure5: Variation of imaginary part (ϵ''_r) of dielectric constant with frequency for at $(\text{Ni}_{0.3} \text{Cu}_{0.20}\text{Zn}_{0.5}) \text{La}_x\text{Fe}_{2-x}\text{O}_4$ different La contents.

B. A.C. conductivity

The A.C. conductivity was evaluated using the relation [22],

$$(9) \dots \sigma_{a.c} = 2\pi f \epsilon_0 \epsilon'_r \tan \delta$$

The variations of the A.C electrical conductivity of bulk $(\text{Ni}_{0.3} \text{Cu}_{0.20}\text{Zn}_{0.5}) \text{La}_x\text{Fe}_{2-x}\text{O}_4$ with frequency is shown in figures 6. It can be noted the A.C conductivity $\sigma_{a.c}(\omega)$ increases with increases in the frequency for all specimens. Which is the normal behaviour of ferrites this agrees with the result of references [24].

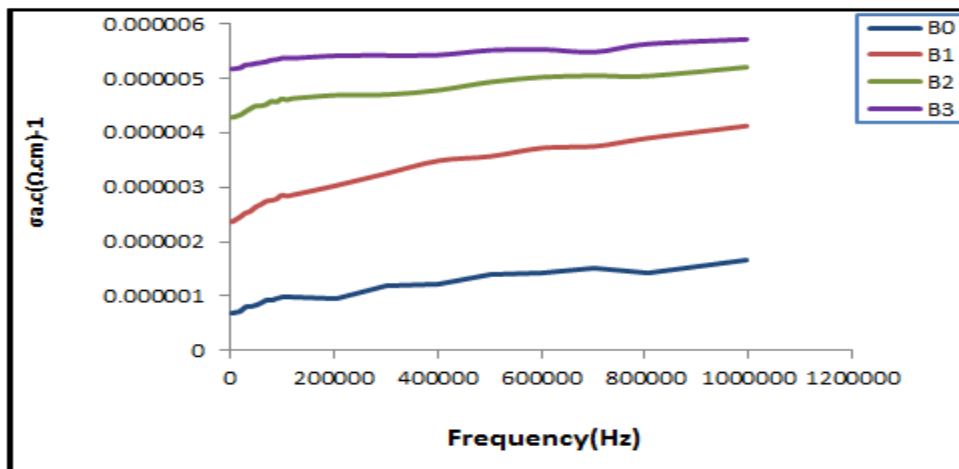


Figure6: A.C electrical conductivity as a function of frequency for with $(\text{Ni}_{0.3} \text{Cu}_{0.20} \text{Zn}_{0.5}) \text{La}_x \text{Fe}_{2-x} \text{O}_4$ different contents of La.

IV. Conclusions

The $(\text{Ni}_{0.3} \text{Cu}_{0.20} \text{Zn}_{0.5}) \text{La}_x \text{Fe}_{2-x} \text{O}_4$ where $(x= 0.0, 0.025, 0.050 \text{ and } 0.075)$ Nano ferrites were prepared using Sol-Gel method. The X-ray diffraction studies clearly showed formations of the crystalline structure of $(\text{Ni}_{0.3} \text{Cu}_{0.20} \text{Zn}_{0.5}) \text{La}_x \text{Fe}_{2-x} \text{O}_4$ is cubic spinel structure phase ferrite and The Average crystallite size (D) was calculated as (23.7-39.5nm) using Williamson's Hall and Debay -shere equation, The lattice parameter is found to increase with increasing lanthanum content. The real and imaginary part of dielectric constant decrease with increasing of frequency, while the A.C electrical conductivity is increased with increasing of frequency.

REFERENCES

- [1] N. S. Gajbhiye and G. Balaji, "Mossbaur studies of nanosized CuFe_2O_4 Ferrites," Advances in Nano science and Nano Tech, A. Sharma, Ed., NISCAIR, 2003.
- [2] S. ManjuraHoque, Md. Amanullah Choudhury and Md. Fakhru Islam, Characterization of Ni-Cu Mixed Spinel Ferrite, *Journal of Magnetism and Magnetic Materials*, 251(3), 2002, 292-303.
- [3] A. Verma, R. Chatterjee, "Effect of zinc concentration on the structural, electrical and magnetic properties of mixed Mn-Zn and Ni-Zn ferrites Synthesized by the citrate precursor technique" *J. Magn. Mater.* Vol. 306, 2006, PP. 313-320.

[4] E. Veena Gopalan, I. A. Al-Omari, K. A. Malini et al., "Impact of zinc substitution on the structural and magnetic properties of chemically derived nanosized manganese zinc mixed ferrites", *J Magn. Mater.* Vol. 321, 2009, PP. 1092-1099.

[5] M. Srivastava, S. Chaubey, A. K. Ojha, "Investigation on size dependent structural and magnetic behavior of nickel ferrite nanoparticles prepared by sol-gel and hydrothermal methods", *Mater. Chem. Phys.* Vol. 118, 2009, PP. 174-180.

[6] P. K. Roy, Bibhuti B. Nayak, J. Bera, "Study on electro-magnetic properties of La substituted Ni-Cu-Zn ferrite synthesized by auto combustion method", *J. Magn. Mater.* Vol. 320, 2008, PP. 1128-1132.

[7] .Shinde TJ, Gadkari AB, Vasambekar PN. Influence of Nd³⁺ substitution on structural, electrical and magnetic properties of nanocrystalline nickel ferrites. *Journal of Alloys and Compounds.* 2012; 513:80±5.

[8] Pervaiz E, Gul I, editors. Influence of rare earth (Gd⁺³) on structural, gigahertz dielectric and magnetic studies of cobalt ferrite. *Journal of Physics: Conference Series*; 2013: IOP Publishing.

[9] P. K. Roy and J. Bera, *J. Magn. Mater.* 298 (2006), pp. 38–42. Abstract | Full Text + Links | PDF (210 K) | Abstract + References in Scopus | Cited By in Scopus.

[10] Zahi S, Hashim M, Daud AR. Synthesis, magnetic properties and microstructure of Ni±Zn ferrite by sol± gel technique. *Journal of Magnetism and Magnetic Materials.* 2007; 308(2):177±82.

[11] Bugad R, Mane T, Navale B, Thombare J, Babar A, Karche B. Structural, morphological and compositional properties of La³⁺ substituted Mg±Zn ferrite interlocked nanoparticles by co-precipitation method, *Journal of Materials Science: Materials in Electronics.* 1±7.

[12] Al Angari Y. Magnetic properties of La-substituted NiFe₂O₄ via egg-white precursor route. *Journal of Magnetism and Magnetic Materials.* 2011; 323(14):1835±9.

[13] Dasan, Y. K., et al. "Influence of La³⁺ Substitution on Structure, Morphology and Magnetic Properties of Nanocrystalline Ni-Zn Ferrite." *PLOS ONE* 12.1 (2017): e0170075.

[14] Cullity BD. *Elements of X-ray Diffraction.* California: Addison – Wesley; 1978.

[15] Gao F, Qin G, Li Y, Jiang Q, Luo L, Zhao K, et al. One-pot synthesis of La-doped SnO₂ layered nanoarrays with an enhanced gas-sensing performance toward acetone. *RSC Advances.* 2016; 6(13):10298±310.

[16] Sutka A, Mezinskis G, Lulis A. Electric and dielectric properties of nanostructured stoichiometric and excess-iron Ni–Zn ferrites. *Phys Scr* 2013; 87: 025601 – 7.

[17] Aghav PS, Dhage VN, Mane ML, Shengule DR, Dorik RG, Jadhav KM. Effect of aluminum substitution on the structural and magnetic properties of cobalt ferrite synthesized by sol–gel auto combustion process. *Phys B* 2011; 406: 4350 – 5.

[18] Wang Y, Xu F, Li L, Liu H, Qiu H, Jiang J. Magnetic properties of La-substituted Ni±Zn±Cr ferrites via rheological phase synthesis. *Materials Chemistry and Physics*. 2008; 112(3):769±73.

[19] Anupama MK, Rudraswamy B. Effect of Gd⁺³Cr⁺³ ion substitution on the structural, electrical and magnetic properties of Ni±Zn ferrite nanoparticles. *IOP Conference Series: Materials Science and Engineering*. 2016; 149(1):012194.

[20]. Rezlescu N, Rezlescu E, Popa P, Rezlescu L. Effects of rare-earth oxides on physical properties of Li± Zn ferrite. *Journal of alloys and compounds*. 1998; 275:657±9.

[21] Roy, P. K., and J. Bera. "Enhancement of the magnetic properties of Ni–Cu–Zn ferrites with the substitution of a small fraction of lanthanum for iron." *Materials research bulletin* 42.1 (2007): 77-83.

[22] Kambale R C, Adhate N R, Chougule B K and Kolekar Y D 2010 *J. Alloys Compd.* 491372.

[23] R. S. Devan, Y .D. Kolekar and B. K. Coagula, "Effect of Cobalt Substitution on The Properties of Nickel–Copper Ferrite" *J. Physics: Condensed Matter*, 18, 2006, 43.

[24] P.A. Noorkhan and S. Kalayne, "Synthesis, Characterization Ac Conductivity of Nickel Ferrite", *Journal of Engineering Research and Applications*, 2, 2012, 681-685.